NJC

Accepted Manuscript

This article can be cited before page numbers have been issued, to do this please use: G. Huang, S. Chen, Q. Qin, J. Luo, M. Tan, Z. Wang, B. Zou and H. Liang, *New J. Chem.*, 2019, DOI: 10.1039/C9NJ01076A.

ROYAL SOCIETY OF CHEMISTRY

rsc.li/njc

New Journal of Chemistry

View Article Online
DOI: 10.1039/C9NJ01076A

ARTICLE

In vitro and *in vivo* activity of novel platinum(II) complexes with naphthalene imide derivatives inhibiting human non-small cell lung cancer cells

Received 00th January 20xx,
Accepted 00th January 20xx

DOI: 10.1039/x0xx00000x

www.rsc.org/

Guo-Bao Huang [a,1], Shan Chen [b,1], Qi-Pin Qin [a,d,*], Jin-Rong Luo [a], Ming-Xiong Tan [a,*], Zhen-Feng Wang [a], Bi-Qun Zou [c,*] and Hong Liang [d,*]

Four new Pt(II) complexes, [Pt(L^a)]Cl (**1**), [Pt(L^b)]Cl (**2**), [Pt(L^c)]Cl (**3**) and [Pt(L^d)]Cl (**04**) with the naphthalene imide derivatives L^a–L^d as ligands were designed and prepared. MTT assay indicated that **1**−**4** exhibited proliferation inhibiting activity against human non-small cell lung cancer (NCI-H460) cells, especially **1**−**3** showed superior activity (IC_{50}= 0.10–8.56 μM) comparing with cisplatin (IC_{50}= 12.01 ± 1.03 μM). Various experiments showed that **3** as a telomerase inhibitor induced NCI-H460 cell apoptosis via inhibition of the telomerase and dysfunction of mitochondria. *In vivo* evaluation results suggested that **03** could significantly inhibit the growth of tumor cells in NCI-H460 tumor-bearing mice and the tumor growth inhibition rate (TGI) reached 40.7%. These results demonstrated that **3** is a telomerase inhibitor and a promising anti-cancer agent.

Introduction

Cisplatin and its derivatives, including oxaliplatin, nedaplatin, carboplatin, heptaplatin, and lobaplatin, are the most frequently used anti-tumor compounds or complexes[1–11]. Unfortunately, some cancer cells frequently develop resistance to cisplatin and its derivatives[11–20], in the course of treatment. Consequently, there are intensive efforts to design new compounds that can overcome drug resistance[11–29]. The investigated compounds include 3-(2′-benzimidazolyl) coumarin Pt(II) complexes[28], peripheral benzodiazepine receptors Pt(II) complexes[29], aqueous arsenous acid Pt(II) anti-cancer complexes[10], and mitochondrion-targeted Pt(II) complex[3]. Recently, luminescent platinum(II) complex [Pt(C^N^Npyr)(C^NR)]$^+$ (HC^N^N^{pyr}=2-phenyl-6-(1H-yrazol-3-yl)-pyridine))[23], *trans,trans,trans*-[$PtCl_2(OH)_2$(isopropylamine)(methylamine) complex[9], *cis,cis,trans*-diamminedichloridodisuccinatoplatinum(IV)-peptide bioconjugates[4], 1,2-bis[2-methyl-5-(4-pyr-idyl)-3-thienyl]-perfluorocyclopentene Pt(II) complex[22], Pt^{IV} prodrugs[25], germinal bisphosphonate moieties Pt(II) compounds[26], and Pt(II)-Gd(III) complex with the [{$Pt(NH_3)_2Cl$}$_2$GdL]$(NO_3)_2$[24] are also investigated.

Moreover, it has been reported that naphthalene and its derivatives exert their anti-cancer activities *via* photoinduced DNA damage, Topoisomerase I/II inhibition, G-quadruplex DNA (G4-DNA) binding, and/or related mechanisms[30,31]. In addition, a series of colorimetric probes for metal ions based on naphthalene derivatives have been reported[32–40]. However, platinum(II) complexes with the naphthalene imide derivatives L^a–L^d as ligands have yet to be reported, and the detailed *in vitro* and *in vivo* anticancer mechanisms of these Pt(II) complexes remain unexplored.

In this work, we synthesized and evaluated four new Pt(II) complexes, [Pt(L^a)]Cl (**1**), [Pt(L^b)]Cl (**2**), [Pt(L^c)]Cl (**3**) and [Pt(L^d)]Cl (**4**) with the naphthalene imide derivatives L^a–L^d as ligands. The effects of these Pt(II) complexes with naphthalene imide derivatives on cell apoptosis were evaluated.

Results and discussion

Synthesis

Four naphthalene imide derivatives including L^a, L^b, L^c and L^d were first prepared *via* the synthetic routes shown in Scheme 1, starting from 3-hydroxy-1,8-naphthalic anhydride. Subsequently, [Pt(L^a)]Cl (**1**), [Pt(L^b)]Cl (**2**), [Pt(L^c)]Cl (**3**) and [Pt(L^d)]Cl (**4**) complexes were obtained by the reaction of L^a–L^d ligands with *cis*-$Pt(DMSO)_2Cl_2$ at 1:1 ratio in 30.0 mL CH_3CN at 80 °C for 6.0 h (Scheme 1). The structures of **1**−**4** and their L^a–L^d ligands were characterized with NMR, IR spectroscopy, ESI-MS, and elemental analysis (Figs. S1−S31). The coordination geometry of Pt(II) atom in **1**−**4** can be described as a four-coordinated (N^N^N-ligand) square planar geometry.

[a] *Guangxi Key Lab of Agricultural Resources Chemistry and Biotechnology, School of Chemistry and Food Science, Yulin Normal University, 1303 Jiaoyudong Road, Yulin 537000, PR China. qpqin2018@126.com (Q.-P. Qin); mxtan2018@126.com (M.-X. Tan). Tel./Fax.: +86-775-2623650.*
[b] *College of physical science and technology, Yulin Normal University, 1303 Jiaoyudong Road, Yulin 537000, PR China.*
[c] *Department of Chemistry, Guilin Normal College, 9 Feihu Road, Gulin 541001, China. zoubiqun@163.com (B.-Q. Zou).*
[d] *State Key Laboratory for the Chemistry and Molecular Engineering of Medicinal Resources, School of Chemistry and Pharmacy, Guangxi Normal University, 15 Yucai Road, Guilin 541004, PR China. hliang@gxnu.edu.cn (H. Liang).*
[1] *These authors contributed equally to this work.*
† Electronic Supplementary Information (ESI) available: The ESI-MS, UV-Vis, IR, and NMR data of each compound in this study. See DOI: 10.1039/x0xx00000x

View Article Online
DOI: 10.1039/C9NJ01076A

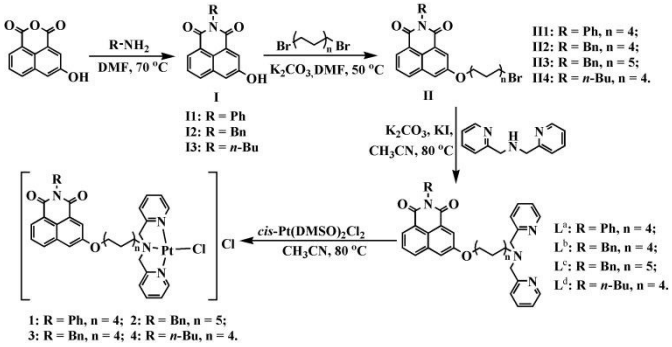

Scheme 1. Synthetic routes for naphthalene imide derivatives L^a–L^d and their complexes **1**–**4**.

Stability of 1–4 in Tris-HCl buffer

The stability of **1**–**4** (4.0×10^{-5} M) in 10 mM Tris-HCl buffer (pH 7.35, containing 2% DMSO) was determined using ESI-MS assays.[40–55] At t = 0 h, the four Pt(II) complexes showed base peaks at m/z = 773.0 (**1**, $[M\text{-}Cl]^+$), 801.1 (**2**, $[M\text{-}Cl]^+$), 786.2 (**3**, $[M\text{-}Cl]^+$) and 753.1 (**4**, $[M\text{-}Cl]^+$), respectively. After 48-h incubation, these peaks of the four Pt(II) complexes were minimally perturbed (Figs. S20–S23), demonstrating that **1**–**4** (4.0×10^{-5} M) were stable in Tris-HCl buffer.

In vitro cytotoxicity

The cytotoxicity of the naphthalene imide derivatives L^a–L^d and their Pt(II) complexes **1**–**4** against human non-small cell lung cancer (NCI-H460) cells, hepatoma cancer (BEL-7402) cells, cervical carcinoma tumor (HeLa) cells, ovarian cancer (SK-OV-3) cells and normal hepatocyte (HL-7702) cells was evaluated by MTT assay with *cis*-$Pt(DMSO)_2Cl_2$ and cisplatin as positive control. For all tested tumor cells, the cytotoxic activities of **1**–**4** were higher than that of the naphthalene imide derivatives L^a–L^d and *cis*-$Pt(DMSO)_2Cl_2$, suggesting the synergistic effect upon the combination of Pt(II) with L^a–L^d ligands. And the *in vitro* cytotoxicity were in the following order: **3** > **1** > **2** > cisplatin > **4** > L^a > L^b > L^c > L^d > *cis*-$Pt(DMSO)_2Cl_2$. In addition, the Pt(II) complexes **1**–**3** showed low IC_{50} values (5.81 ± 0.36 μM for **1**, 8.56 ± 1.01μM for **2**, and 0.10 ± 0.15 μM for **3**) on NCI-H460 cancer cells, which indicated they were 3.5–150.3 times more cytotoxic than the naphthalene imide derivatives L^a–L^d ligands, and 1.4–120.1 times more cytotoxic than cisplatin (IC_{50}= 12.01 ± 1.03 μM). Importantly, **3** has remarkably anti-cancer activity against NCI-H460 cells and its anti-cancer activity against NCI-H460 cell line was higher than or close to previous reports complexes.[32–40] Compared with HL-7702 normal cells, the IC_{50} values of **1**–**4** toward the NCI-H-460 cells was enhanced by 3.2–650.3 times, suggesting the selectivity of **1**–**4** on NCI-H460 cells.

Table 1. IC_{50}[a] (μM) values of the naphthalene imide derivatives L^a–L^d and **1**–**4** against the five tested human cells.

Compounds	NCI-H460	BEL-7402	HeLa	SK-OV-3	HL-7702
L^a	29.61 ± 0.74	22.15 ± 1.22	18.39 ± 0.29	15.11 ± 0.34	30.24 ± 0.82
1	5.81 ± 0.36	5.88 ± 1.06	10.94 ± 1.78	6.05 ± 0.57	62.14 ± 1.57
L^b	30.11 ± 1.53	25.01 ± 1.09	19.32 ± 0.18	17.64 ± 1.09	32.09 ± 1.06
2	8.56 ± 1.01	10.51 ± 1.03	17.03 ± 1.11	9.33 ± 1.36	59.33 ± 0.35
L^c	15.33 ± 1.44	20.15 ± 0.93	16.33 ± 0.75	12.03 ± 1.02	28.66 ± 1.06
3	0.10 ± 0.15	3.56 ± 1.69	7.03 ± 1.52	1.99 ± 0.33	65.03 ± 1.05
L^d	31.59 ± 1.82	27.17 ± 1.37	20.74 ± 1.64	25.33 ± 1.29	35.02 ± 1.97
4	18.87 ± 1.26	20.33 ± 0.45	25.10 ± 1.03	19.02 ± 1.14	60.02 ± 1.02
cis-$Pt(DMSO)_2Cl_2$	>150	>150	>150	>150	>150
cisplatin [b]	12.01 ± 1.03	14.06 ± 1.58	15.59 ± 0.24	16.14 ± 1.09	17.88 ± 1.01

[a] IC_{50} values was the compound/complex concentration effective in inhibiting 50% of the cell growth measured by the MTT assay at 24.0 h, which were presented as the mean ± SD (standard deviation of the mean value) from six independent assays. [b] 1.0 mM Cisplatin was dissolved in 0.154 M NaCl[50–56].

Complex 3 inhibited telomerase *via* down-regulating the hTERT and c-myc proteins

Recent studies demonstrated that telomerase is present in the majority (85-90%) of tumor cells[57–63], which is restricted by the level of hTERT and c-myc proteins[57–65]. Thus, to confirm whether **3** (0.10 μM) and **4** (18.87 μM) exerted their anti-tumor activities through telomerase inhibition, their mechanisms of actions were evaluated by a modified TRAP assay in NCI-H460 cells. Complex **3** showed potent inhibitory activity (IR= 53.60%) against telomerase at 0.10 μM (Fig. 1A), higher than that of **4** (18.87 μM, 6.13%). As expected, **3** (0.10 μM) showed a significantly decrease in hTERT and c-myc activity, differing

View Article Online
DOI: 10.1039/C9NJ01670A

from **4** (18.87 μM) in this study (Fig. 1B and C), which agreed with the results of telomerase inhibition assays.

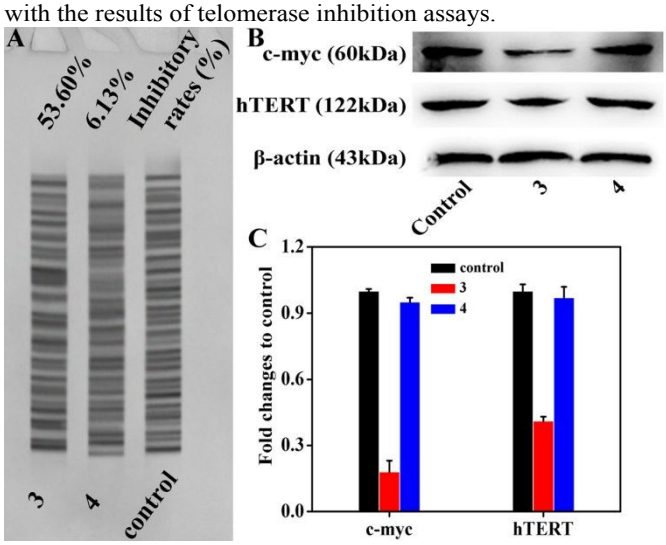

Fig. 1 Pt(II) complex **3** (0.10 μM) inhibited telomerase *via* down-regulating the hTERT and c-myc proteins. (A) Telomerase inhibition by **3** (0.10 μM) and **4** (18.87 μM). (B) The levels of hTERT/c-myc in NCI-H460 cells after treated with **3** (0.10 μM) and **4** (18.87 μM) for 24 h. (C) The same blots were stripped and reprobed with a β-actin antibody to show equal protein loading. Western blotting bands from three independent measurements were quantified with Image J. in (C).

Tumor cell apoptosis induced by 3 and 4

The apoptotic activities of **3** (0.10 μM) and **4** (18.87 μM) were assessed using flow cytometry (FCM) with Annexin V/PI (Propidium idodine) staining in NCI-H460 cancer cells. Results indicated that **3** (0.10 μM) exhibited significant apoptosis (75.4%) in NCI-H460 tumor cells as compared with **4** (15.0%) and control (3.7%) (Fig. 2), which was higher than or close to previous reports complexes.[32–40] These results also suggested **3** (0.10 μM) and **4** (18.87 μM) induced NCI-H460 cell death mainly through apoptosis.

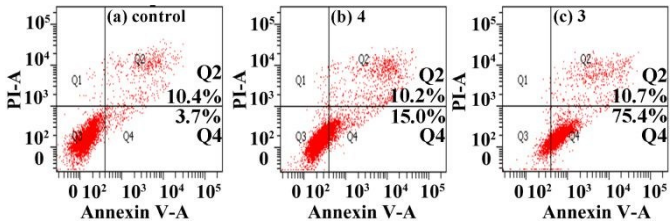

Fig. 2 The induction of apoptosis in NCI-H460 cells after treated with **3** (0.10 μM) and **4** (18.87 μM) for 24 h.

Expression of apoptosis related-proteins induced by 3 and 4

Disruption of mitochondrial functions is a potential mechanism for Pt(II) compounds to exert their cytotoxicity to tumor cells[65–72]. In addition, the FCM analyses results suggested that **3** (0.10 μM) and **4** (18.87 μM) induced apoptosis in NCI-H460 cells (Fig. 2). The NCI-H460 cell apoptosis was further investigated by measuring the protein levels. We found that the apoptosis proteins levels of anti-apoptotic apaf-1 and cytochrome c (cyt c) were significantly increased by **3** (0.10 μM), while bcl-2 protein was concurrently decreased (Fig. 3). However, **4** (18.87 μM) did not display such obvious effects on the change of apoptosis proteins in NCI-H460 cells.

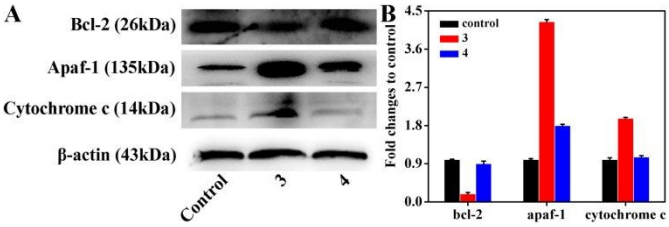

Fig. 3 (A) The effects of **3** (0.10 μM) and **4** (18.87 μM) on the apoptosis-related proteins in NCI-H460 cells. (B) The same blots were stripped and reprobed with a β-actin antibody to show equal protein loading. Western blotting bands from three independent measurements were quantified with Image J. in (B). The control group cells were treated with vehicle (1% DMSO).

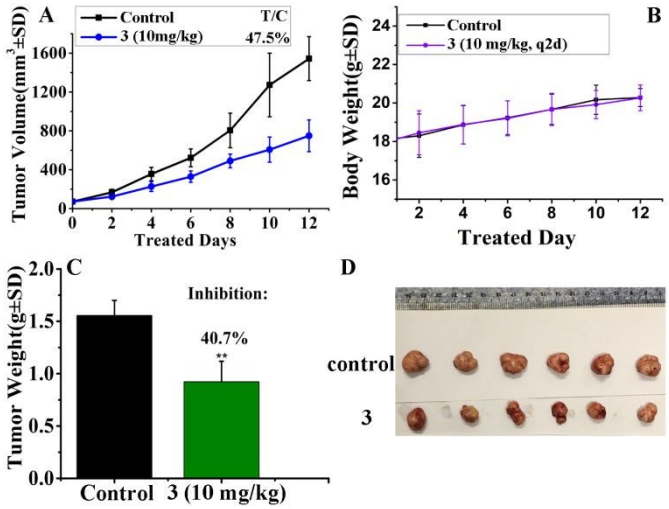

Fig. 4 *In vivo* anti-cancer activity of **3** (10.0 mg/kg every 2 days (q2d)) in mice bearing NCI-H460 tumor xenograft. (A) Effect of **3** (10.0 mg/kg/q2d) and vehicle (5% DMSO in saline, v/v) on growth of NCI-H460 tumor xenograft (n= 6). (B) Body weight change (%). (C) The mice tumor weight, (**) $P < 0.05$, p vs the vehicle control group. (D) Photographs of NCI-H460 tumor from the experimental group.

Evaluation of anti-cancer activity *in vivo*

To understand the inhibitory activity of complex **3** on the growth of cancer/tumor cells *in vivo*, NCI-H460 models were selected to evaluate the anti-cancer effects of **3**. Thus, nude mice bearing NCI-H460 cell xenografts were treated with **3** dosed at 10.0 mg/kg every 2 days (q2d)) in solvent (5% v/v DMSO/saline, 1.0 mL/20 g) through intraperitoneal injection, along with vehicle (5% DMSO in saline, v/v) treatment.[73–80] No significant toxicity was observed in **3** treated (10.0 mg/kg/q2d) mice. The results indicated that **3** significantly decreased the

View Article Online
DOI: 10.1039/C9NJ01075A

tumor weights of NCI-H460 xenograft mouse model (Fig. 4 and Tables S1–S3). The tumor growth inhibition (TGI) rate of 3 was 40.7%, which was much higher than that of cisplatin (TGI= 25.5%)[76,79,80].

Conclusions

In this study, four new Pt(II) complexes, [Pt(L^a)]Cl (**1**), [Pt(L^b)]Cl (**2**), [Pt(L^c)]Cl (**3**) and [Pt(L^d)]Cl (**4**) with naphthalene imide derivatives L^a–L^d as ligands were prepared and biologically evaluated as potential antitumor agents. Among the 4 complexes, **3** exhibited potent proliferation inhibiting activities against NCI-H460, BEL-7402, HeLa and SK-OV-3 cells (IC_{50}= 0.10–7.03μM). Further experiments showed that **03** induced NCI-H460 cell apoptosis via inhibition of the telomerase and dysfunction of mitochondria. *In vivo* studies demonstrated that **3** (10.0 mg/kg/q2d) displayed potent anti-cancer activity with TGI of 40.7% in NCI-H460 tumor-bearing mice. Taken together, **3** is a promising anti-cancer agent and a telomerase inhibitor.

Experimental methods

Synthesis of naphthalene imide derivatives L^a–L^d

Synthesis of compound I

3-Hydroxy-1,8-naphthalic anhydride (640 mg, 3 mmol) was dissolved in DMF (100 mL). The amine (15 mmol) was added and the resulting mixture was stirred at 70 °C for 1-3 h. DMF was removed in *vacuo*, and the remaining residue was dissolved in water and stirred for 1 h. After removing water by filtration and the remaining residue was washed with water for several times, solubilized in methanol and filtered, the combined organic layers were dried over Na_2SO_4 and filtered. The residue was obtained after removal of solvents in vacuum, which was purified by chromatography to give the product compound **I** as a yellow solid.

Synthesis of compound II

K_2CO_3 (280 mg, 2.0 mmol) was added to a solution of compound **I** (1.0 mmol) in DMF (20 mL). After stirring for 0.5 h, bromide alkane (10.0 mmol) was added and the resulting mixture was stirred at 50 °C for 18 h. DMF was removed in *vacuo*, and the remaining residue was dissolved in water and stirred for 1 h. After removing water by filtration and the remaining residue was washed with water for several times, solubilized in methanol and filtered, the combined organic layers were dried over Na_2SO_4 and filtered. After removal of the solvents *in vacuo,* purification by chromatography gave the product compound **II** as a yellow solid.

Synthesis of L^a–L^d ligands

K_2CO_3 (170 mg, 1.25 mmol) and KI (210mg, 1.25 mmol) were added to a solution of compound **2** (0.25 mmol) in CH_3CN (20 mL). After stirring for 0.5 h, 2, 2-dipicolyamine (150 mg, 0.75 mmol) was added and the resulting mixture was stirred at 80 °C for 18 h. After removal of the solvents *in vacuo,* purification by chromatography gave the product compound **3** as a yellow solid (Scheme 1).

Data for 5-hydroxy-2-phenyl-1H-benzo[de]isoquinoline-1,3(2H)-dione (**I1**). Yield = 98.0 %. ^{1}H NMR (400 MHz, DMSO-d_6) δ 10.55 (s, 1H), 8.32-8.23 (m, 2H), 8.03 (d, J = 2.5 Hz, 1H), 7.85-7.74 (m, 1H), 7.71 (d, J = 2.4 Hz, 1H), 7.57-7.49 (m, 2H), 7.48-7.44 (m, 1H), 7.42-7.34 (m, 2H).

Data for 5-(4-bromobutoxy)-2-phenyl-1H-benzo[de]isoquinoline-1,3(2H)-dione (**II2**). Yield = 38.0 %. ^{1}H NMR (400 MHz, DMSO-d_6) δ 8.45-8.26 (m, 2H), 8.04-7.97 (m, 2H), 7.86-7.79 (m, 1H), 7.53 (t, J = 7.4 Hz, 2H), 7.46 (t, J = 7.2 Hz, 1H), 7.43-7.33 (m, 2H), 4.28 (t, J = 6.1 Hz, 2H), 3.65 (t, J = 6.5 Hz, 2H), 2.12-1.85 (m, 4H).

Data for 5-(4-(bis(pyridin-2-ylmethyl)amino)butoxy)-2-phenyl-1H-benzo[de]isoquinoline-1,3(2H)-dione (L^a). Yield = 51.0 %. ^{1}H NMR (400 MHz, $CDCl_3$) δ 8.53 (d, J = 4.6 Hz, 2H), 8.47 (dd, J = 7.3, 1.0 Hz, 1H), 8.22 (d, J = 2.5 Hz, 1H), 8.11 (d, J = 7.6 Hz, 1H), 7.72 (dd, J = 8.1, 7.5 Hz, 1H), 7.66 (t, J = 7.0 Hz, 2H), 7.61-7.52 (m, 4H), 7.52-7.45 (m, 2H), 7.32 (dd, J = 5.3, 3.3 Hz, 2H), 7.21-7.12 (m, 2H), 4.09 (t, J = 6.0 Hz, 2H), 3.92 (s, 4H), 2.75-2.78 (m, 2H), 1.91-1.86 (m, 4H). ^{13}C NMR (101 MHz, $CDCl_3$) δ 164.4, 164.0, 157.7, 149.0, 136.4, 135.4, 133.4, 132.8, 129.4, 128.9, 128.7, 128.6, 127.4, 124.1, 123.9, 123.2, 123.0, 122.6, 122.0, 113.9, 68.4, 60.4, 53.7, 26.7, 23.6.

Data for 2-benzyl-5-hydroxy-1H-benzo[de]isoquinoline-1,3(2H)-dione (**I2**). Yield = 69.0 %. ^{1}H NMR (400 MHz, DMSO-d_6) δ 8.28-8.25 (m, 2H), 8.05 (d, J = 2.5 Hz, 1H), 7.75 (dd, J = 8.2, 7.3 Hz, 1H), 7.67 (d, J = 2.4 Hz, 1H), 7.39-7.26 (m, 5H), 5.23 (s, 2H).

Data for 2-benzyl-5-(4-bromobutoxy)-1H-benzo[de]isoquinoline-1,3(2H)-dione (**II2**).Yield = 75.0 %. ^{1}H NMR (400 MHz, $CDCl_3$) δ 8.44 (d, J = 7.2 Hz, 1H), 8.25 (d, J = 2.5 Hz, 1H), 8.05 (d, J = 8.1 Hz, 1H), 7.68 (t, J = 7.8 Hz, 1H), 7.54 (d, J = 7.3 Hz, 2H), 7.50 (d, J = 2.5 Hz, 1H), 7.30 (t, J = 7.4 Hz, 2H), 7.26-7.21 (m, 1H), 5.37 (s, 2H), 4.19 (t, J = 5.8 Hz, 2H), 3.52 (t, J = 6.3 Hz, 2H), 2.17-1.98 (m, 4H).

Data for 2-benzyl-5-(4-(bis(pyridin-2-ylmethyl)amino)butoxy)-1H-benzo[de]isoquinoline-1,3(2H)-dione (L^b). Yield = 78.0 %. ^{1}H NMR (400 MHz, $CDCl_3$) δ 8.48 (d, J = 4.9 Hz, 2H), 8.39 (d, J = 7.2 Hz, 1H), 8.16 (d, J = 2.5 Hz, 1H), 7.99 (d, J = 8.2 Hz, 1H), 7.72-7.57 (m, 3H), 7.55-7.48 (m, 4H), 7.39 (d, J = 2.4 Hz, 1H), 7.34-7.24 (m, 2H), 7.24-7.18 (m, 1H), 7.14-7.04 (m, 2H), 5.34 (s, 2H), 4.04-4.01 (m, 2H), 2.63 (t, J = 7.0 Hz, 2H), 1.93-1.80 (m, 2H), 1.78-1.70 (m, 2H). ^{13}C NMR (101 MHz, $CDCl_3$) δ 164.3, 163.9, 157.5, 137.3, 133.2, 132.7, 129.0, 128.9, 128.5, 127.5, 127.5, 124.1, 123.7, 122.8, 122.5, 113.9, 100.0, 67.6, 43.6, 33.3, 32.6, 31.0, 29.3, 27.7.

Data for 2-benzyl-5-((5-bromopentyl)oxy)-1H-benzo[de]isoquinoline-1,3(2H)-dione (**II3**). Yield = 61.0 %. ^{1}H NMR (400 MHz, $CDCl_3$) δ 8.44 (d, J = 7.2 Hz, 1H), 8.25 (d, J = 2.5 Hz, 1H), 8.05 (d, J = 8.1 Hz, 1H), 7.68 (t, J = 7.8 Hz, 1H), 7.54 (d, J = 7.3 Hz, 2H), 7.50 (d, J = 2.5 Hz, 1H), 7.30 (t, J = 7.4 Hz, 2H), 7.26-7.21 (m, 1H), 5.37 (s, 2H), 4.19 (t, J = 5.8 Hz, 2H), 3.52 (t, J = 6.3 Hz, 2H), 2.17-1.98 (m, 4H).

Data for 2-benzyl-5-((5-(bis(pyridin-2-ylmethyl)amino)pentyl)oxy)-1H-benzo[de]isoquinoline-1,3(2H)-

dione (L^{c}). Yield = 70.0 %. ^{1}H NMR (400 MHz, $CDCl_3$) δ 8.48 (d, J = 4.9 Hz, 2H), 8.39 (d, J = 7.2 Hz, 1H), 8.16 (d, J = 2.5 Hz, 1H), 7.99 (d, J = 8.2 Hz, 1H), 7.72-7.57 (m, 3H), 7.55-7.48 (m, 4H), 7.39 (d, J = 2.4 Hz, 1H), 7.34-7.24 (m, 2H), 7.24-7.18 (m, 1H), 7.14-7.04 (m, 2H), 5.34 (s, 2H), 4.04-4.01 (m, 2H), 2.63 (t, J = 7.0 Hz, 2H), 1.93-1.80 (m, 2H), 1.78-1.70 (m, 2H). ^{13}C NMR (101 MHz, $CDCl_3$) δ 164.3, 163.9, 157.5, 137.3, 133.2, 132.7, 129.0, 128.9, 128.5, 127.5, 127.5, 124.1, 123.7, 122.8, 122.5, 113.9, 100.0, 67.6, 43.6, 33.3, 32.6, 31.0, 29.3, 27.7.

Data for 2-butyl-5-hydroxy-1H-benzo[de]isoquinoline-1,3(2H)-dione (**I3**). Yield = 95.0 %. ^{1}H NMR (400 MHz, DMSO-d_6) δ 7.83 (dd, J = 11.7, 4.5 Hz, 2H), 7.61 (d, J = 2.4 Hz, 1H), 7.32 (dd, J = 8.1, 7.4 Hz, 1H), 7.23 (d, J = 2.4 Hz, 1H), 3.75-3.46 (m, 2H), 1.34-1.11 (m, 2H), 1.03-0.87 (m, 2H), 0.52 (t, J = 7.4 Hz, 3H).

Data for 5-(4-bromobutoxy)-2-butyl-1H-benzo[de]isoquinoline-1,3(2H)-dione (**II4**). Yield = 82.0 %. ^{1}H NMR (400 MHz, $CDCl_3$) δ 8.43 (d, J = 7.3 Hz, 1H), 8.24 (d, J = 2.5 Hz, 1H), 8.06 (d, J = 8.2 Hz, 1H), 7.69 (t, J = 7.8 Hz, 1H), 7.50 (d, J = 2.4 Hz, 1H), 4.38-4.01 (m, 4H), 3.53 (t, J = 6.3 Hz, 2H), 2.20-1.99 (m, 4H), 1.75-1.67 (m, 2H), 1.49-1.40 (m, 2H), 0.98 (t, J = 7.3 Hz, 3H).

Data for 5-(4-(bis(pyridin-2-ylmethyl)amino)butoxy)-2-butyl-1H-benzo[de]isoquinoline-1,3(2H)-dione (L^{d}). Yield = 67.0 %. ^{1}H NMR (400 MHz, $CDCl_3$) δ 8.50-8.48 (m, 2H), 8.39 -8.36 (m, 1H), 8.15 (dd, J = 2.4, 1.7 Hz, 1H), 8.00 (d, J = 8.3 Hz, 1H), 7.66-7.59 (m, 3H), 7.51 (d, J = 7.7 Hz, 2H), 7.40 (s, 1H), 7.14-7.04 (m, 2H), 4.13 (dd, J = 15.0, 7.4 Hz, 2H), 4.05 (dd, J = 15.2, 9.1 Hz, 2H), 2.63 (t, J = 7.0 Hz, 2H), 1.89-1.82 (m, 2H), 1.78-1.65 (m, 4H), 1.54-1.36 (m, 2H), 0.95 (t, J = 7.3 Hz, 3H). ^{13}C NMR (101 MHz, $CDCl_3$) δ 164.3, 163.9, 159.8, 157.7, 149.0, 136.4, 133.2, 132.42, 128.4, 127.3, 124.0, 123.5, 123.0, 122.7, 122.6, 122.0, 113.6, 68.4, 60.5, 53.8, 40.3, 26.8, 23.6, 20.4, 13.9.

Synthesis of 1−4

Four Pt(II) complexes **1**−**4** were obtained by the reaction of L^{a}–L^{d} ligands with *cis*-Pt(DMSO)$_2$Cl$_2$ at a 1.0:1.0 ratio in 30.0 mL CH_3CN at 80 °C for 6.0 h (Scheme 1).

Data for **1**. Yield: 85.3%. ESI-MS: *m*/*z* = 773.0 [M-Cl]$^{+}$. IR (KBr): 3403, 2934, 1703, 1662, 1626, 1487, 1438, 1377, 1338, 1279, 1248, 1222, 1165, 1185, 1106, 880, 781, 767, 697, 546, 440 cm^{-1}. ^{1}H NMR (600 MHz, DMSO-d_6) δ 8.75 (d, *J* = 5.5 Hz, 2H), 8.30 (t, *J* = 8.3 Hz, 2H), 8.25 (t, *J* = 8.2 Hz, 2H), 7.84 (s, 1H), 7.82 (s, 2H), 7.80 (d, *J* = 9.0 Hz, 2H), 7.61 (t, *J* = 6.6 Hz, 2H), 7.54 (t, *J* = 7.5 Hz, 2H), 7.47 (s, 1H), 7.39 (d, *J* = 7.2 Hz, 2H), 5.40 (d, *J* = 15.8 Hz, 2H), 4.88 (d, *J* = 15.8 Hz, 2H), 4.08 (s, 2H), 3.15 (s, 2H), 1.75 (s, 4H). ^{13}C NMR (151 MHz, DMSO-d_6) δ 165.83, 163.67, 163.22, 156.69, 148.98, 141.27, 135.96, 133.15, 133.09, 129.06, 128.88, 128.22, 128.09, 127.67, 125.31, 123.96, 123.43, 123.20, 122.39, 121.74, 113.96, 67.80, 67.74, 63.82, 40.39, 25.29, 23.80. Elemental analysis calcd. (%) for $C_{34}H_{30}Cl_2N_4O_3Pt$: C 50.50, H 3.74, N 6.93; found: C 50.45, H 3.76, N 6.90.

Data for **2**. Yield: 80.6%. ESI-MS: *m*/*z* = 801.1 [M-Cl]$^{+}$. IR (KBr): 3400, 2937, 1698, 1659, 1624, 1439, 1331, 1271, 1162, 1009, 959, 781, 747, 526, 505, 439 cm^{-1}. ^{1}H NMR (600 MHz, DMSO-d_6) δ 8.76 (d, *J* = 5.5 Hz, 2H), 8.30 (d, *J* = 7.2 Hz, 1H), 8.26 (d, *J* = 8.1 Hz, 3H), 7.89 (s, 1H), 7.80 (s, 2H), 7.78 (d, *J* = 7.5 Hz, 2H), 7.63 (t, *J* = 6.7 Hz, 2H), 7.35 (d, *J* = 7.5 Hz, 2H), 7.30 (t, *J* = 7.5 Hz, 2H), 7.23 (t, *J* = 7.3 Hz, 1H), 5.36 (d, *J* = 15.8 Hz, 2H), 5.22 (s, 2H), 4.85 (d, *J* = 15.9 Hz, 2H), 4.04 (s, 2H), 3.06 (s, 2H), 1.64 (s, 2H), 1.60 (s, 2H), 1.39 (s, 2H). ^{13}C NMR (151 MHz, DMSO-d_6) δ 165.81, 163.46, 163.07, 156.86, 149.01, 141.27, 137.27, 133.17, 133.09, 128.35, 128.29, 127.69, 127.51, 127.07, 125.30, 123.41, 123.29, 122.76, 121.98, 121.71, 114.00, 68.09, 67.82, 64.08, 42.93, 40.39, 27.93, 26.70, 22.65. Elemental analysis calcd. (%) for $C_{36}H_{34}Cl_2N_4O_3Pt$: C 51.68, H 4.10, N 6.70; found: C 51.65, H 4.14, N 6.68.

Data for **3**. Yield: 90.1%. ESI-MS: *m*/*z* = 786.2 [M-Cl]$^{+}$. IR (KBr): 3408, 2925, 1698, 1584, 1440, 1329, 1272, 1163, 978, 780, 731, 705, 525, 508 cm^{-1}. ^{1}H NMR (600 MHz, DMSO-d_6) δ 8.75 (d, *J* = 5.6 Hz, 2H), 8.30 (d, *J* = 7.2 Hz, 1H), 8.24 (d, *J* = 8.6 Hz, 3H), 7.81 (d, *J* = 9.1 Hz, 3H), 7.78 (d, *J* = 7.8 Hz, 2H), 7.59 (t, *J* = 6.6 Hz, 2H), 7.36 (d, *J* = 7.7 Hz, 2H), 7.31 (t, *J* = 7.4 Hz, 2H), 7.24 (t, *J* = 7.2 Hz, 1H), 5.38 (d, *J* = 15.8 Hz, 2H), 5.23 (s, 2H), 4.86 (d, *J* = 15.8 Hz, 2H), 4.05 (s, 2H), 3.14 (s, 2H), 1.74 (s, 4H). ^{13}C NMR (151 MHz, DMSO-d_6) δ 165.86, 163.51, 163.07, 156.77, 149.04, 141.31, 137.34, 133.23, 133.07, 128.43, 127.77, 127.59, 127.15, 125.34, 123.47, 123.30, 122.82, 121.95, 121.74, 114.22, 67.87, 67.77, 63.89, 43.00, 40.42, 25.33, 23.87. Elemental analysis calcd. (%) for $C_{35}H_{32}Cl_2N_4O_3Pt$: C 51.10, H 3.92, N 6.81; found: C 51.05, H 3.95, N 6.79.

Data for **4**. Yield: 88.2%. ESI-MS: *m*/*z* = 753.1 [M-Cl]$^{+}$. IR (KBr): 3411, 2955, 1699, 1659, 1625, 1439, 1383, 1334, 1272, 1162, 1071, 780, 549, 440 cm^{-1}. ^{1}H NMR (600 MHz, DMSO-d_6) δ 8.76 (d, *J* = 5.5 Hz, 2H), 8.31 (d, *J* = 8.0 Hz, 1H), 8.26 (t, *J* = 7.7 Hz, 3H), 7.83 (s, 1H), 7.82 – 7.77 (m, 4H), 7.61 (t, *J* = 6.6 Hz, 2H), 5.34 (d, *J* = 15.8 Hz, 2H), 4.84 (d, *J* = 15.8 Hz, 2H), 4.07 (s, 2H), 4.04 (t, *J* = 7.4 Hz, 2H), 3.14 (s, 2H), 1.74 (s, 4H), 1.62 (s, 2H), 1.36 (d, *J* = 7.5 Hz, 2H), 0.93 (t, *J* = 7.4 Hz, 3H). ^{13}C NMR (151 MHz, DMSO-d_6) δ 165.78, 163.40, 162.98, 156.74, 149.02, 141.28, 133.02, 132.92, 128.11, 127.70, 125.32, 123.51, 123.40, 122.78, 121.93, 121.71, 113.90, 67.84, 67.68, 63.80, 40.39, 29.62, 25.29, 23.80, 19.77, 13.70. Elemental analysis calcd. (%) for $C_{32}H_{34}Cl_2N_4O_3Pt$: C 48.74, H 4.35, N 7.10; found: C 48.70, H 4.37, N 7.08.

Methods and evaluation

The *in vitro* and *in vivo* anti-tumor activities of **3** and **4** were evaluated and analyzed according to Metzler-Nolte, Liang, Chao and Lippard *et al*. reported[44,45,51,69,76−80]. In addition, the detailed experimental methods were described in the Electro Supporting Information Materials.

Acknowledgements

We thank the National Natural Science Foundation of China (Nos. 21867017, 21861014 and 21761033), the Natural Science Foundation of Guangxi (Nos. 2018GXNSFBA138021,

2017GXNSFBA198211, 2018GXNSFAA294064 and 2018GXNSFBA281188), the Yulin Normal University Research Grant (Nos. 2018YJKY36, 201810606010 and 201810606083), the Innovative Team & Outstanding Talent Program of Colleges and Universities in Guangxi (2014-49 and 2017-38) as well as the scientific research project of Guilin Normal College (KYA201804) for the financial support.

Notes and references

1 Q. Cao, Y. Li, E. Freisinger, P. Z. Qin, R. K. O. Sigela and Z.-W. Mao, *Inorg. Chem. Front.*, 2017, **4**, 10−32.
2 Z.-F. Chen, Q.-P. Qin, J.-L. Qin, J. Zhou, Y.-L. Li, N. Li, Y.-C. Liu and H. Liang, *J. Med. Chem.*, 2015, **58**, 4771−4789.
3 K. Wang, C. Zhu, Y. He, Z. Zhang, W. Zhou, N. Muhammad, Y. Guo, X. Wang and Z. Guo, *Angew. Chem. Int. Edit.*, 2019, **58**, 4638–4643.
4 L. Gaviglio, A. Gross, N. Metzler-Nolte and M. Ravera, *Metallomics*, 2012, **4**, 260–266.
5 T. Meng, Q.-P. Qin, Z.-L. Chen, H.-H. Zou, K. Wang and F.-P. Liang, *Dalton Trans.*, 2019, **48**, 5352–5360.
6 J. Liu, C.-H. Leung, A. L.-F. Chow, R. W.-Y. Sun, S.-C. Yan and C.-M. Che, *Chem. Commun.*, 2011, **47**, 719–721.
7 H. Baruah, C. G. Barry and U. Bierbach, *Curr. Top. Med. Chem.*, 2004, **4**, 1537–1549.
8 X. Han, J. Sun, Y. Wang and Z. He, *Med. Res. Rev.*, 2015, **35**, 1268–1299.
9 L. Cubo, T. W. Hambley, P. J. S. Miguel, A. Carnero, C. Navarro-Ranninger and A. G. Quiroga, *Dalton Trans.*, 2011, **40**, 344–347.
10 Đ. U. Miodragović, J. A. Quentzel, J. W. Kurutz, C. L. Stern, R. W. Ahn, I. Kandela, A. Mazar and T. V. O'Halloran, *Angew. Chem. Int. Ed.*, 2013, **52**, 1–5.
11 B. Rosenberg, L. Vancamp, J. E. Trosko and V. H. Mansour, *Nature*, 1969, **222**, 385–386.
12 Z. H. Siddik, *Oncogene*, 2003, **22**, 7265–7279.
13 L. Kelland, *Nat. Rev. Cancer*, 2007, **7**, 573–584.
14 N. J. Wheate, S. Walker, G. E. Craig and R. Oun, *Dalton Trans.*, 2010, **39**, 8113–8127.
15 D. Wang and S. J. Lippard, *Nat. Rev. Drug Discovery*, 2005, **4**, 307–320.
16 N. Graf and S. J. Lippard, *Adv. Drug Delivery Rev.*, 2012, **64**, 993–1004.
17 A. Casini and J. Reedijk, *Chem. Sci.*, 2012, **3**, 3135–3144.
18 A. Emadi and S. D. Gore, *Blood Rev.*, 2010, **24**, 191–199.
19 X.-W. Zhang, X.-J. Yan, Z.-R. Zhou, F.-F. Yang, Z.-Y. Wu, H.-B. Sun, W.-X. Liang, A.-X. Song, V. Lallemand-Breitenbach, M. Jeanne, Q.-Y. Zhang, H.-Y. Yang, Q.-H. Huang, G.-B. Zhou, J.-H. Tong, Y. Zhang, J.-H. Wu, H.-Y. Hu, H. de The, S.-J. Chen and Z. Chen, *Science*, 2010, **328**, 240–243.
20 H. Chen, W. He and Z. Guo, *Chem. Commun.*, 2014, **50**, 9714–9717.
21 K. B. Garbutcheon-Singh, P. Leverett, S. Myers and J. R. Aldrich-Wright, *Dalton Trans.*, 2013, **42**, 918–926.
22 A. Presa, R. F. Brissos. A. B. Caballero, I. Borilovic, L. Korrodi-Gregório, R. Pérez-Tomás, O. Roubeau, P. Gamez, *Angew. Chem. Int. Ed.*, 2015, **54**, 4561–4565.
23 J. L.-L. Tsai, T. Zou, J. Liu, T. Chen, A. O.-Y. Chan, C. Yang, C.-N. Lok and C.-M. Che, Chem. Sci., 2015, 6, 3823–3830.
24 Z. Zhu, X. Wang, T. Li, S. Aime, P. J. Sadler and Z. Guo, *Angew. Chem. Int. Ed.*, 2014, **126**, 13441–13444.
25 J. S. Butler and P. J. Sadler, *Curr. Opin. Chem. Biol.*, 2013, 17:175–188.
26 Z. Xue, M. Lin, J. Zhu, J. Zhang, Y. Li and Z. Guo, *Chem. Commun.*, 2010, 46, 1212–1214.
27 T. Lazarević, A. Rilak and Ž. D. Bugarčić, *Eur. J. Med. Chem.*, 2017, 142, 8–31.
28 T. Meng, Q.-P. Qin, Z.-R. Wang, L.-T. Peng, H.-H. Zou, Z.-Y. Gan, M.-X. Tan, K. Wang and F.-P. Liang, *J. Inorg. Biochem.*, 2018, **189**, 143–150.
29 N. Margiotta, N. Denora, R. Ostuni, V. Laquintana, A. Anderson, S. W. Johnson, G. Trapani and G. Natile, *J. Med. Chem.*, 2010, **53**, 5144–5154.
30 X. Xu, S. Wang, Y. Chang, C. Ge, X. Li, Y. Feng, S. Xie, C. Wang, F. Dai and W. Luo, *Med. Chem. Commun.*, 2018, **9**, 1377–1385.
31 M. D. Tomczyk and K. Z. Walczak, *Eur. J. Med. Chem.*, 2018, **159**, 393−422.
32 M. J. Chang and M. H. Lee, *Dyes and Pigments*, 2018, **149**, 915–920.
33 H. Wang, L. Yang, W. Zhang, Y. Zhou, B. Zhao, X. Li, *Inorg. Chim. Acta*, 2012, **381**, 111–116.
34 C. Zhang, Z. Liu, Y. Li, W. He, X. Gao and Z. Guo, *Chem. Commun.*, 2013, **49**, 11430–11432.
35 J. Fan, Y. Wu and X. Peng, *Chem. Lett.*, 2004, **33**, 1392–1393.
36 E. E. Langdon-Jones, N. O. Symonds, S. E. Yates, A. J. Hayes, D. Lloyd, R. Williams, S. J. Coles, P. N. Horton and S. J. A. Pope, *Inorg. Chem.*, 2014, **53**, 3788−3797.
37 S. Y. Kim and J.-I. Hong, *Tetrahedron Lett.*, 2009, **50**, 2822–2824.
38 E. E. Langdon-Jones, A. B. Jones, C. F. Williams, A. J. Hayes, D. Lloyd, H. J. Mottram and S. J. A. Pope, *Eur. J. Inorg. Chem.*, 2017, 759–766.
39 R. Seliga, M. Pilatova, M. Sarissky, V. Viglasky, M. Walko, J. Mojzis, *Mol. Biol. Rep.*, 2013, **40**, 4129–4137.
40 J. F. Zhang, M. Park, W. X. Ren, Y. Kim, S. J. Kim, J. H. Jung and J. S. Kim, *Chem. Commun.*, 2011, **47**, 3568–3570.
41 A. Zamora, S. A. Pérez, V. Rodríguez, C. Janiak, G. S. Yellol and J. Ruiz, *J. Med. Chem.*, 2015, **58**, 1320−1336.
42 A. M. Krause-Heuer, R. Grünert, S. Kühne, M. Buczkowska, N. J. Wheate, D. D. Le Pevelen, L. R. Boag and D. M. Fisher, *J. Med. Chem.*, 2009, **52**, 5474–5484.
43 Q.-P. Qin, T. Meng, M.-X. Tan, Y.-C. Liu, X.-J. Luo, B.-Q. Zou and H. Liang, *Eur. J. Med. Chem.*, 2018, **143**, 1597−1603.
44 Y. Gothe, T. Marzo, L. Messori and N. Metzler-Nolte, *Chem. Eur. J.*, 2016, **22**, 1−9.
45 Y. Gothe, T. Marzo, L. Messori and N. Metzler-Nolte, *Chem. Eur. J.*, 2016, **22**, 12487−12494.
46 Y.-R. Zheng, K. Suntharalingam, T. C. Johnstone and Stephen J. Lippard, *Chem. Sci.*, 2015, **6**, 1189−1193.
47 D. Y. Q. Wong, J. Y. Lau and W. H. Ang, *Dalton Trans.*, 2012, **41**, 6104−6111.
48 H. M. Coley, J. Sarju and G. Wagner, *J. Med. Chem.*, 2008, **51**, 135−141.
49 K.-H. Leung, H.-Z. He, B. He, H.-J. Zhong, S. Lin, Y.-T. Wang, D.-L. Ma and C.-H. Leung, *Chem. Sci.*, 2015, **6**, 2166–2171.
50 A. Briš, J. Jašík, I. Turel and J. Roithová, *Dalton Trans.*, 2019, **48**, 2626–2634.
51 Q.-P. Qin, S.-L. Wang, M.-X. Tan, Z.-F. Wang, X.-L. Huang, Q.-M. Wei, B.-B. Shi, B.-Q. Zou and H. Liang, *Metallomics*, 2018, **10**, 1160–1169.
52 H. Huang, P. Zhang, B. Yu, Y. Chen, J. Wang, L. Ji and H. Chao, *J. Med. Chem.*, 2014, **57**, 8971–8983.
53 Q.-P. Qin, S.-L. Wang, M.-X. Tan, Z.-F. Wang, D.-M. Luo, B.-Q. Zou, Y.-C. Liu, P.-F. Yao and H. Liang, *Eur. J. Med. Chem.*, 2018, **158**, 106−122.
54 Q.-P. Qin, S.-L. Wang, M.-X. Tan, Y.-C. Liu, T. Meng, B.-Q. Zou and H. Liang, *Eur. J. Med. Chem.*, 2019, **161**, 334−342.
55 H. Yua , S. Gou, Z. Wang, F. Chen and L. Fang, *Eur. J. Med. Chem.*, 2016, **114**, 141−152.

View Article Online
DOI: 10.1039/C9NJ01076A

56 R. Cao, J.-L. Jia, X.-C. Ma, M. Zhou and H. Fei, *J. Med. Chem.*, 2013, **56**, 3636−3644.
57 A. Paul, B. Maji, S. K. Misra, A. K. Jain, K. Muniyappa and S. Bhattacharya, *J. Med. Chem.*, 2012, **55**, 7460−7471.
58 T.-M. Ou, Y.-J. Lu, J.-H. Tan, Z.-S. Huang, K.-Y. Wong and L.-Q. Gu, *ChemMedChem*, 2008, **3**, 690−713.
59 B.-S. Herbert, G. C. Gellert, A. Hochreiter, K. Pongracz,W. E. Wright, D. Zielinska, A. C. Chin, C. B. Harley, J. Wshay and S. M. Gryaznov, *Oncogene*, 2005, *24*, 5262–5268.
60 K. Dhaene, E. Van Marck and R. Parwaresch, *Virchows Arch.*, 2000, **437**, 1–16.
61 M. Meyerson, *J. Clin. Oncol.*, 2000, **18**, 2626–2634.
62 A.-L. Ducrest, H. Szutorisz, J. Lingner and M. Nabholz, *Oncogene*, 2002, **21**, 541–552.
63 P. A. Waghorn, M. R. Jackson, V. Gouverneur and K. A. Vallis, Eur. J. Med. Chem., 2017, 125, 117–129.
64 Y. Wang, F.-X. Cheng, X.-L. Yuan, W.-J. Tang, J.-B. Shi, C.-Z. Liao and X.-H. Liu, *Eur. J. Med. Chem.*, 2016, **112**, 231–251.
65 Q.-P. Qin, B.-Q. Zou, M.-X. Tan, S.-L. Wang, Y.-C. Liu and H. Liang, *New J. Chem.*, 2018, **42**, 15479–15487.
66 V. T. Yilmaz, C. Icsel, O. R. Turgut, M. Aygun, M. Erkisa, M. H. Turkdemir and E. Ulukaya, *Eur. J. Med. Chem.*, 2018, **155**, 609–622.
67 Q.-P. Qin, Z.-F. Chen, J.-L. Qin, X.-J. He, Y.-L. Li, Y.-C. Liu, K.-B. Huang and H. Liang, *Eur. J. Med. Chem.*, 2015, **92**, 302–313.
68 S. P. Wisnovsky, J. J. Wilson, R. J. Radford, M. P. Pereira, M. R. Chan, R. R. Laposa, S. J. Lippard and S. O. Kelley, *Chem. Biol.*, 2013, **20**, 1323–1328.
69 K. Suntharalingam, J. J. Wilson, W. Lin and S. J. Lippard, *Metallomics*, 2014, **6**, 437–443.
70 S. Fulda, L. Galluzzi and G. Kroemer, *Nat. Rev. Drug Discov.*, 2010, **9**, 447–464.
71 F.-U. Rahman, M. Z. Bhatti, A. Ali, H.-Q. Duong, Y. Zhang, B. Yang, S. Koppireddi, Y. Lin, H. Wang, Z.-T. Li and D.-W. Zhang, *Eur. J. Med. Chem.*, 2018, **143**, 1039–1052.
72 Y. Li, Z. Gu, C. Zhang, S. Li, L. Zhang, G. Zhou, S. Wang and J. Zhang, *Eur. J. Med. Chem.*, 2018, **144**, 662–671.
73 S. Göschl, E. Schreiber-Brynzak, V. Pichler, K. Cseh, P. Heffeter, U. Jungwirth, M. A. Jakupec, W. Berger and B. K. Keppler, *Metallomics*, 2017, **9**, 309−322.
74 A. Weiss, R. H. Berndsen, M. Dubois, C. Muller, R. Schibli, A. W. Griffioen, P. J. Dyson and P. Nowak-Sliwinska, *Chem. Sci.*, 2014, **5**, 4742–4748.
75 J. Yan, J. Chen, S. Zhang, J. Hu, L. Huang and X. Li, *J. Med. Chem.*, 2016, **59**, 5264–5283.
73 F. Dai, Q. Li, Y. Wang, C. Ge, C. Feng, S. Xie, H. He, X. Xu and C. Wang, *J. Med. Chem.*, 2017, **60**, 2071–2083.
76 Z.-F. Chen, Q.-P. Qin, J.-L. Qin, Y.-C. Liu, K.-B. Huang, Y.-L. Li, T. Meng, G.-H. Zhang, Y. Peng, X.-J. Luo and H. Liang, *J. Med. Chem.*, 2015, **58**, 2159−2179.
77 J. B. Shi, L. Z. Chen, Y. Wang, C. Xiou, W. J. Tang, H. P. Zhou, X. H. Liu and Q. Z. Yao, *Eur. J. Med. Chem.*, 2016, **124**, 729–739.
78 J.-Q. Wang, P.-Y. Zhang, L.-N. Ji and H. Chao, *J. Inorg. Biochem.*, 2015, **146**, 89–96.
79 T. Meng, Q.-P. Qin, Z.-L. Chen, H.-H. Zou, K. Wang and F.-P. Liang, *Eur. J. Med. Chem.*, 2019, **169**, 103–110.
80 Q.-P. Qin, Z.-F. Wang, S.-L. Wang, D.-M. Luo, B.-Q. Zou, P.-F. Yao, M.-X. Tan and H. Liang, *Eur. J. Med. Chem.*, 2019, **170**, 195–202.

View Article Online
DOI: 10.1039/C9NJ01076A

Graphical abstract

In vitro and *in vivo* activity of novel platinum(II) complexes with naphthalene imide derivatives inhibiting human non-small cell lung cancer cells

Guo-Bao Huang [a,1], Shan Chen [b,1], Qi-Pin Qin [a,d,*], Jin-Rong Luo [a], Ming-Xiong Tan [a,*], Zhen-Feng Wang [a], Bi-Qun Zou [c,*] and Hong Liang [d,*]

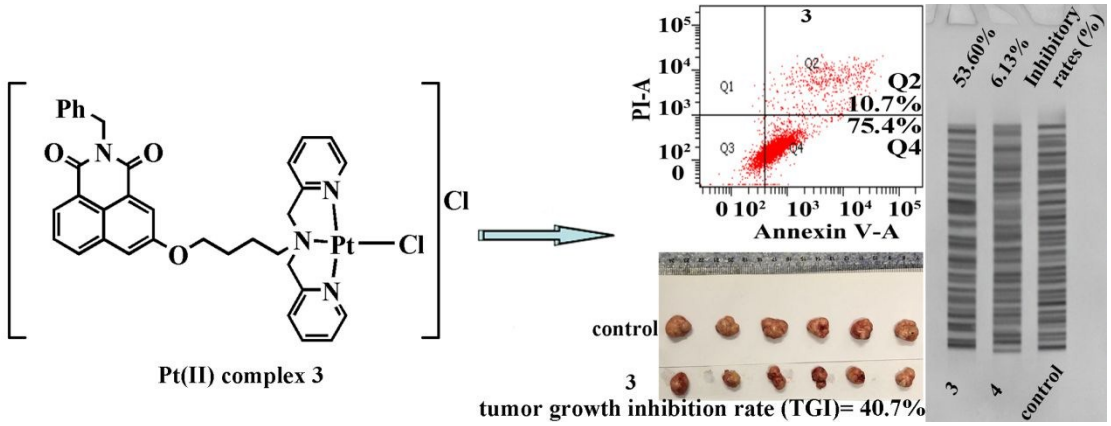

3 induced NCI-H460 cell apoptosis via inhibition of the telomerase and dysfunction of mitochondria. Remarkably, **3** obviously inhibited NCI-H460 xenograft tumor growth *in vivo*.